

Bonding Interactions in Olefin (C₂X₄, X = H, F, Cl, Br, I, CN) Iron Tetracarbonyl Complexes: Role of the Deformation Energy in Bonding and Reactivity

David L. Cedeño and Eric Weitz*

Department of Chemistry, Northwestern University, Evanston, Illinois 60208-3113

Attila Bérces†

Steacie Institute for Molecular Science, National Research Council of Canada,
Ottawa, Ontario K1A 0R6, Canada

Received: April 12, 2001; In Final Form: June 14, 2001

The iron–olefin bond energies for the monoolefin iron tetracarbonyl complexes Fe(CO)₄(C₂X₄) (X = H, F, Cl, Br, I, CN) have been determined using density functional theory (DFT), with the BP86 functional. An energy decomposition analysis of the bonding interactions demonstrate that, as predicted by current models of metal–olefin bonding, the attractive electronic interactions of the haloolefins and percyanoethylene with iron are stronger than those of ethylene. However, in addition to these electronic interactions the net bond energy depends on the energy needed to deform the Fe(CO)₄ and olefin moieties from their equilibrium geometries to the geometrical conformation they adopt in the complex. This energy is termed the deformation energy. As a result of the deformation energy, the bond energies for the substituted olefins are similar to or smaller than that of the Fe–C₂H₄ bond. More than half of the total deformation energy involves deforming the olefin, principally as a result of a change in hybridization of the carbon atoms from sp² in the free olefin toward an sp³-like carbon in the bound olefin. The deformation of Fe(CO)₄ involves mainly the axial CO ligands, which bend away from the olefin as a result of a repulsive interaction with the olefin substituents. In addition, the increase in the C–X bond length, upon bonding of the olefin to Fe(CO)₄, correlates well with the exothermicity of the oxidative addition reaction, Fe(CO)₄(C₂X₄) → XFe(CO)₄(C₂X₃), indicating that the deformation of the bound olefin lowers the energy of the C–X bond.

Introduction

In general, both stoichiometric and catalytic reactions of organometallic complexes involve breaking and forming metal–ligand bonds. Therefore, an evaluation of the thermodynamics of such reactions requires knowledge of metal–ligand bond energies (BDEs). The experimental determination of metal–ligand BDEs in organometallic complexes is often difficult.¹ However, it has been demonstrated that density functional theory (DFT) has advanced to the point where such calculations can be a reliable source of bond energies in these complexes.^{2–4} In many cases bond energies calculated using DFT, with the BP86 functional, are within a few kcal/mol of the experimental values.^{5–13} Calculations of bond energies can also provide insights into the factors that contribute to the overall bond energy and their relative importance. One such method involves an energy decomposition scheme,^{14–16} in which the bond energy is decomposed into an algebraic sum of attractive and repulsive interactions, which are both electronic and steric in nature. This energy decomposition analysis, in combination with an analysis of the change in population of the interacting orbitals of the metal and the ligand, can be a very useful tool for understanding the factors that determine the net bond energy.^{13,14,16}

Olefin complexes of metal carbonyls have long been of interest. They participate in a variety of catalytic reactions including olefin isomerization, hydrosilation, hydrogenation, and

hydroformylation.^{17–20} The reaction paths and yields of these processes can be dependent on the stability of the olefin–metal bond. Further, the Dewar–Chatt–Duncanson (DCD) model^{21,22} is a generally accepted model that is used to describe the olefin–metal bond. According to this model, the bond has contributions from two distinct interactions: σ donation from the ligand π orbital to the metal and π back-donation from the metal to the ligand π^* orbital. On the basis of statements in Dewar's original paper²¹ and interpretations of the DCD model by other authors,^{18,23} the prevailing expectation is that the replacement of the hydrogens on ethylene by more electron withdrawing substituents will lead to an *increase* in the metal–ligand interaction because the back-bonding capability of the ligand is increased, provided, as is usually assumed, the σ -donating capability of the ligand is not strongly effected. However, it has been recognized that in some cases the stabilities of mono- and/or dihalogenated olefin complexes are similar to or even lower than those of the analogous ethylene complexes.²³ Although some authors have recognized that steric factors could contribute to a trend in the stability of such complexes, only a few studies have been directed at validating or quantifying this hypothesis.^{24–26} Prior calculations done in our laboratory,²⁷ involving the haloolefin complexes Fe(CO)₄(C₂X₄) (X = F, Cl), indicated that the Fe–haloolefin bond is *similar to or perhaps even weaker* than the Fe–C₂H₄ bond in Fe(CO)₄(C₂H₄) and that this decreased bond energy can be rationalized by the increased deformation energy required to deform the planar olefin and the unsaturated metal carbonyl moiety into the conformations

† Present address: Novartis Forschungsinstitut GmbH, A-1235 Vienna, Austria.

they adopt in the complex. Although a number of monoolefin iron tetracarbonyl complexes have been spectroscopically characterized,^{28–35} and lower limits have been established for the bond enthalpies for $\text{Fe}(\text{CO})_4(\text{C}_2\text{Cl}_4)$ and $\text{Fe}(\text{CO})_4(\text{C}_2\text{F}_4)$,³⁵ the only iron tetracarbonyl–olefin complex for which there is a quantitative and specific experimental determination of the bond enthalpy is $\text{Fe}(\text{CO})_4(\text{C}_2\text{H}_4)$.³⁶

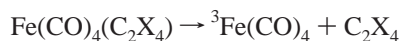
It has also been shown that oxidative addition, for at least some of the substituted olefin complexes, is a possible reaction pathway. Haszeldine and co-workers³⁰ reported the formation of iron tetracarbonyl vinyl halides ($\text{XFe}(\text{CO})_4(\text{C}_2\text{X}_3)$) from the monohaloolefin ($\text{Fe}(\text{CO})_4(\text{C}_2\text{X}_4)$) compounds. However, the reaction has only been reported for $\text{X} = \text{Br}$ and Cl . Cedeño and Weitz^{35c} found that the lowest energy pathway for the unimolecular decay of $\text{Fe}(\text{CO})_4(\text{C}_2\text{Cl}_4)$ is via the oxidative addition channel, rather than direct dissociative loss of the olefin ligand, which is the lowest energy pathway for decomposition of $\text{Fe}(\text{CO})_4(\text{C}_2\text{H}_4)$ ^{31,35a} and $\text{Fe}(\text{CO})_4(\text{C}_2\text{F}_4)$.^{35a}

The objective of this paper is to investigate the bonding interactions between $\text{Fe}(\text{CO})_4$ and a series of olefins, C_2X_4 ($\text{X} = \text{H}, \text{F}, \text{Cl}, \text{Br}, \text{I}, \text{CN}$). The halogens are chosen because they provide a series in which there is a gradual change in both the electron-withdrawing nature and the size of the substituent. The cyano group is included in this series since it is a strong electron-withdrawing group, comparable to the halogens. The interactions are analyzed using an energy decomposition analysis, as well as the degree of orbital overlap, and the change in the Mulliken electron population of the ligand and metal fragment upon bonding. Changes in geometry that occur on bonding are analyzed in terms of the metal–ligand interactions, with an emphasis on their effect on the stability of these complexes and on the reactivity of the complexes toward oxidative addition of the substituted olefin.

Computational Method

Geometries and energies were calculated with the Jaguar³⁷ quantum chemistry program using the pseudospectral method.³⁸ All calculations were performed using density functional theory and the local density approximation (LDA), with the exchange $\text{X}\alpha$ potential by Slater³⁹ and the correlation method of Vosko, Wilk, and Nusair (VWN).⁴⁰ Nonlocal density functionals were added self-consistently. Becke's 88⁴¹ was used for exchange and Perdew's 86⁴² for correlation. The LACV3P** basis set was used. It uses Hay and Wadt's effective core potential (ECP)⁴³ basis set for iron. For other atoms, LACV3P** uses the 6-311G** basis set.⁴⁴ The frozen core approximation was used, in which the outermost core orbitals were included.

Bond energies (ΔE_c) were calculated as the difference in the optimized energies of products and reactants for the reaction



$$\text{X} = \text{H}, \text{F}, \text{Cl}, \text{Br}, \text{I}, \text{CN}$$

$$\Delta E_c = E[{}^3\text{Fe}(\text{CO})_4] + E[\text{C}_2\text{X}_4] - E[\text{Fe}(\text{CO})_4(\text{C}_2\text{X}_4)] \quad (1)$$

Bond energies were calculated relative to the triplet state of $\text{Fe}(\text{CO})_4$ because this is the experimentally determined ground state.⁴⁵ The energy, ΔE_c , represents the reaction energy for olefin dissociation. Thus, by definition those factors that increase bonding interactions are positive. The bond enthalpy at 298 K can be calculated using the expression⁴⁶

$$\Delta H_{298} = \Delta E_c + \Delta \text{ZPE} + \Delta E_{\text{th}} + \Delta(PV) \quad (2)$$

TABLE 1: Calculated Fe– C_2X_4 Bond Energies and Enthalpies for $\text{Fe}(\text{CO})_4(\text{C}_2\text{X}_4)$ ^a

param	X =		
	H	F	Cl
ΔE_c	34.7	37.6	25.3
ΔZPE	–5.0	–2.9	–0.8
$\Delta E_{\text{th}} + \Delta(PV)$	1.7	0.8	0.4
BSSE	–2.7	–7.9	–7.9
ΔH_{298} (with BSSE)	28.7	27.6	17.0
ΔH_{298} (w/out BSSE)	31.4	35.5	24.9
ΔH_{exp}	37 ± 3^b	$> 26^c$	$> 21^d$

^a Energies in kcal/mol. ^b Reference 36. ^c Reference 35a. ^d Reference 35c.

ΔZPE is the zero point vibrational energy change obtained from vibrational frequency calculations. ΔE_{th} is the change associated with the translational, rotational, and vibrational energy in going from 0 to 298 K. $\Delta(PV)$ is the molar work, which is equal to ΔnRT (0.6 kcal/mol at 298 K), assuming ideal gas behavior. Table 1 lists the calculated bond energies and enthalpies for $\text{X} = \text{H}, \text{F},$ and Cl using the LACV3P** basis set, as well as available experimental data. Also listed is the basis set superposition error (BSSE) correction obtained from a counterpoise calculation.⁴⁷ We note the following regarding the BSSE correction. First, the BSSE correction for the $\text{Fe}(\text{CO})_4(\text{C}_2\text{Cl}_4)$ and $\text{Fe}(\text{CO})_4(\text{C}_2\text{F}_4)$ complexes is unusually large.⁷ Second, inclusion of the BSSE correction in the calculation of the BDE decreases the Fe– C_2H_4 bond enthalpy to a point where it is significantly below the experimental value. It also decreases the calculated BDE for $\text{Fe}(\text{CO})_4(\text{C}_2\text{Cl}_4)$ to well below the experimentally determined lower limit, and the calculated BDE for $\text{Fe}(\text{CO})_4(\text{C}_2\text{F}_4)$ is now very close to the minimum value consistent with experiment. Similar behavior with regard to inclusion of the BSSE correction is observed in the series of chromium–olefin complexes, where more experimental data are available.⁴⁸ These observations suggest that either or both of the following factors may contribute to this phenomenon. It is possible that there is a significant error due to truncation of the basis set. This error is expected to be of sign opposite to that of the counterpoise correction.^{7,49} Such an error would effectively negate some or all of the BSSE correction. Additionally, it is possible there is simply a systematic error in the calculated bond energies for these complexes as calculated using DFT methodology. However, we point out that previous calculations^{6,13,27} on iron-containing complexes have demonstrated that DFT calculations using either the B3LYP or the BLYP functional can give bond energies that are even lower than those obtained with the BP86 functional used here. Though these are interesting observations and are worthy of further study, such studies are not the focus of this paper. Thus, we emphasize that what we are most interested in is the trend in bond energies in the series of Fe–olefin complexes under study. As seen in Table 1, the trend in the Fe– C_2H_4 BDE relative to the Fe– C_2F_4 and Fe– C_2Cl_4 BDEs is that the Fe– C_2F_4 BDE is predicted to be either slightly larger or comparable to the Fe– C_2H_4 BDE and in either case the Fe– C_2Cl_4 BDE is smaller than the BDE of either of these complexes with or without inclusion of the BSSE correction.

The bond energy decomposition analysis was performed using the Amsterdam density functional program (ADF99).⁵⁰ It is based on an extended transition state method.^{14,15} All energy decomposition analyses were performed using the same BP86 functional used for energy minimization, and the geometries obtained with Jaguar. When using ADF the atomic orbitals on iron, bromine, and iodine were described by an uncontracted

TABLE 2: Geometries for Olefin Tetracarbonyl Complexes^a

param	X =							
	H	H(expt) ^b	F	F(expt) ^c	Cl	Br	I	CN
Fe–C _{olef}	2.130	2.117	2.016	1.989	2.054	2.030	2.049	2.091
Fe–C _{ax}	1.801	1.796	1.816	1.823	1.822	1.826	1.826	1.833
Fe–C _{eq}	1.784	1.836	1.811	1.846	1.810	1.813	1.811	1.810
C–O _{ax}	1.154		1.148		1.147	1.147	1.148	1.144
C–O _{eq}	1.157		1.152		1.151	1.151	1.152	1.148
C–C _{olef}	1.414	1.46	1.453	1.530	1.465	1.450	1.444	1.488
C–X	1.090	1.08 ^e	1.359	1.336	1.794	1.993	2.195	1.439
C _{ax} –Fe–C _{ax}	177.4		180.8		187.9	188.5	191.4	186.4
C _{eq} –Fe–C _{eq}	113.7		109.0		111.7	113.2	115.2	108.8
Fe–C–O _{ax}	179.9		176.4		173.8	172.8	171.0	174.8
Fe–C–O _{eq}	179.8		177.7		178.7	177.6	177.8	179.6
X–C–X	114.2		109.0		108.7	107.1	106.3	113.6
Θ ^d	26.8	0 ^e	44.8	41.6	42.2	42.8	41.0	33.5

^a Bond lengths in Å; angles in deg. ^b Reference 54. ^c Reference 55. ^d Indicates deviation from planarity, which is defined as the difference between 180° and the X–C–C–X dihedral angle in the bound olefin (Θ is zero for the free olefin). ^e Arbitrarily fixed during the determination.

triple-ζ STO basis set,⁵¹ while a double-ζ STO basis set was used for carbon, nitrogen, oxygen, fluorine, and chlorine. A single-ζ polarization function was used for all atoms. The frozen core approximation^{50b} was used for all atoms (except hydrogens). A set of auxiliary s, p, d, f, g, and h STO functions, centered on all nuclei, was used in order to fit the molecular density and accurately represent the Coulomb and exchange potentials in each SCF cycle.⁵²

The bond energy can be decomposed into contributions from three terms:

$$\Delta E = \Delta E_{oi} + \Delta E_{steric} + \Delta E_{def} \quad (3)$$

ΔE_{def} is the energy necessary to deform the bonding moieties from their respective isolated equilibrium geometries into the geometries they assume in the bound complex. ΔE_{steric} is the sum of two terms, one corresponding to the electrostatic interaction (ΔE_{elst}) between the fragments and the other to the Pauli repulsion energy (ΔE_{pauli}). ΔE_{oi} is the energy due to the interactions between occupied orbitals of one fragment and empty orbitals of the other fragment, as well as between the occupied and empty orbitals within a given fragment (polarization). ΔE_{oi} can be decomposed into a sum of terms, with a term for each irreducible representation of the interacting orbitals. Additionally, for each system, a Mulliken population analysis⁵³ was performed to evaluate the electron population changes occurring when the ligand and metal fragment interact. When one complex is compared to another, some of the calculated energy differences are within the error limits of the level of theory used. However, we focus on *trends* in bond energies and the contributions of various factors to these bond energies.

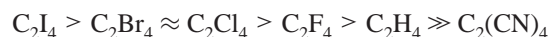
Results and Discussion

A. Geometries of the Fe(CO)₄(C₂X₄) Complexes. The calculated geometries of the Fe(CO)₄(C₂X₄) complexes are shown in Table 2. Comparison with experimental data is possible only for the ethylene⁵⁴ and the perfluoroethylene⁵⁵ complexes. The metal–olefin bond is calculated to be 0.01–0.03 Å longer than the experimental values, while the Fe–C_{ax} bond lengths are calculated to be very close to the experimental values. The largest difference between calculations and experiments involves the Fe–C_{eq} bond length, which is calculated to be 0.05 and 0.04 Å shorter than the experiment values for X = H and F, respectively. Such differences between experiment and theory are not unusual. In general, theory predicts equatorial Fe–C bond lengths to be shorter than axial Fe–C bond

lengths,^{6,9,13} contrary to what is found experimentally. The C–C bond lengths in the olefins are calculated to be 0.05 and 0.08 Å shorter than the experimental values for X = H and F, respectively. Independent of these differences, the agreement between theory and experiment for both bond lengths and bond angles is good. The other halogenated complexes have calculated geometries that are closer to that of Fe(CO)₄(C₂F₄) than Fe(CO)₄(C₂H₄). The Fe–olefin bond lengths in these complexes are shorter than in the ethylene complex. Compared to Fe(CO)₄(C₂F₄) the Fe–olefin bond lengths are longer, with the exception of the Fe–olefin bond length in Fe(CO)₄(C₂Br₄), which is calculated to be similar to the Fe–olefin bond length in Fe(CO)₄(C₂F₄). The C–C olefin bond length is also longer for all the halogenated complexes than for the ethylene complex. But, when compared to the perfluoro complex, only the C–C bond length in Fe(CO)₄(C₂Cl₄) is longer. As will be discussed in the following sections, these trends can be related to the electron-accepting and -donating capabilities of the olefin ligands.

B. Metal–Olefin Bonding Interaction. Scheme 1 shows a picture of the frontier molecular orbitals (FMOs) on the metal fragment and the olefin that are involved in bonding, as well as the minimum energy geometries of the complexes of interest. Only the equatorial (C_{2v} symmetry) isomer of the complexes has been considered since it is well documented from both experiment^{32,34,54,55} and theory⁵⁶ that this isomer is expected to be lowest in energy.

Figure 1 shows the energy of the LUMO and HOMO for each ligand and for the Fe(CO)₄ metal fragment. Relative to ethylene, the energy of the HOMO of the halogenated ligands increases very little (0.2–0.5 eV), while that of percyanoethylene is much lower (~2.5 eV). However, the small increase in the energy of the halogenated olefin ligand's HOMO puts them closer in energy to the metal fragment's LUMO, which should, in principle, slightly improve the σ-donating character of the ligand. It is also clear that C₂(CN)₄ should be the poorest σ-donor, because its HOMO energy is well below that of ethylene and the haloethylenes. Then, solely on the basis of the olefin HOMO–metal LUMO energy gap, the σ-donating capability of the ligands would be expected to decrease in the order



On the other hand, the decrease in the LUMO energy of the other olefins relative to ethylene is large compared to the

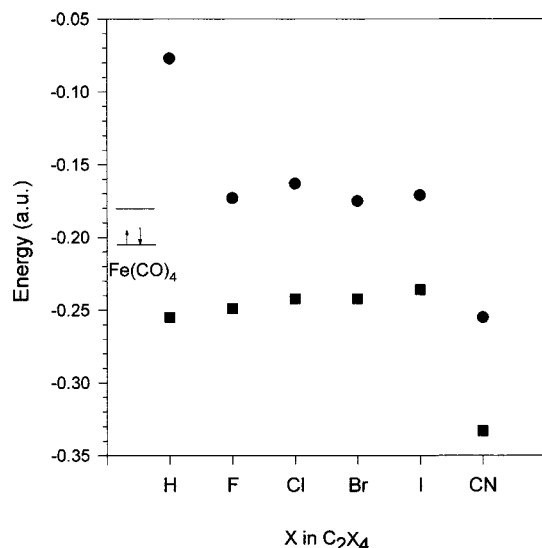


Figure 1. HOMO (■) and LUMO (●) energies for the C₂X₄ moieties (X = H, F, Cl, Br, I, CN) in relation to the energy of the frontier molecular orbitals of Fe(CO)₄.

change in their HOMO energies. The change in the LUMO energy is ~ 2.5 eV for halogenated olefins and ~ 4.8 eV for percyanoethylene, relative to ethylene. The decrease in the LUMO energy of these olefins puts them closer to the HOMO energy of the metal fragment. Indeed, the LUMO in percyanoethylene is *lower* in energy than the HOMO of the Fe(CO)₄ fragment, such that C₂(CN)₄ should be the best π -accepting ligand. On the basis of the olefin LUMO–metal HOMO energy, the back-bonding ability of the substituted olefins should be greater than that of ethylene and should

SCHEME 1

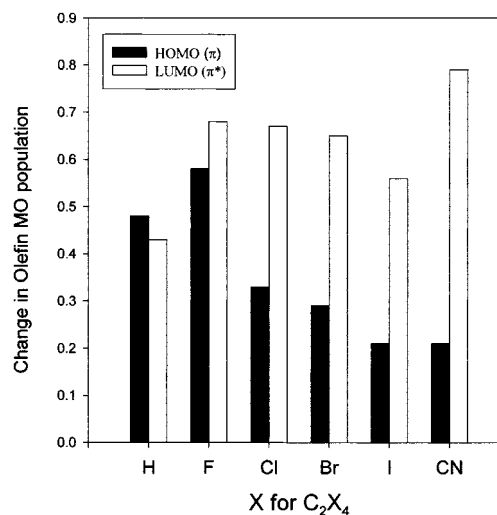
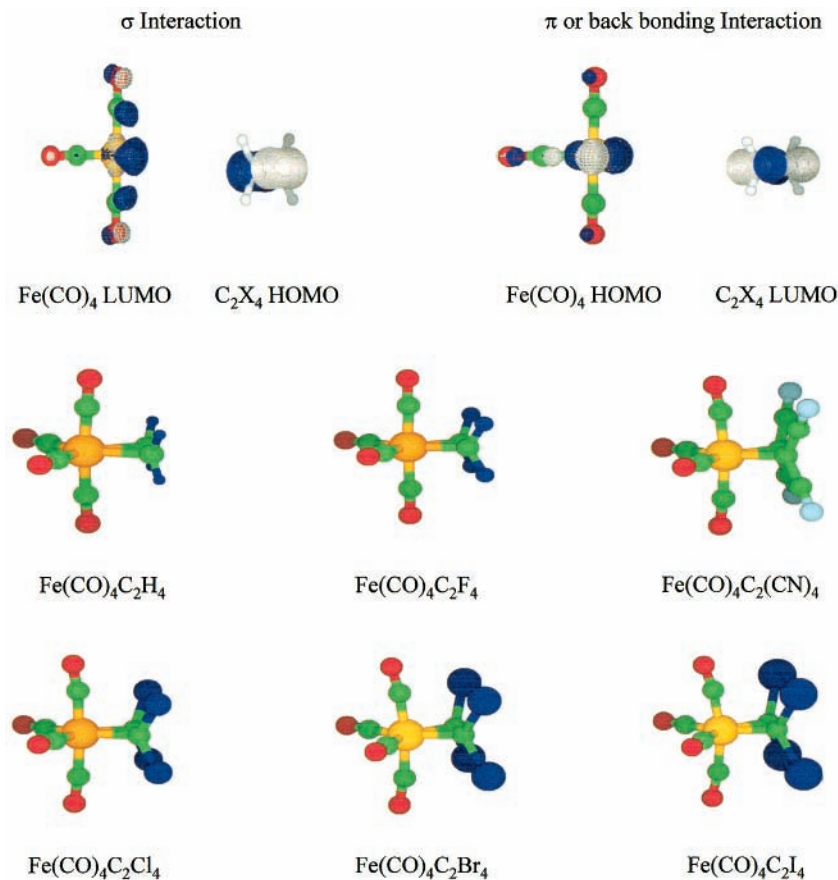
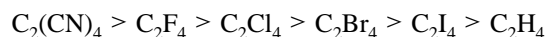


Figure 2. Changes in the absolute value of the olefin HOMO and LUMO Mulliken populations upon bonding to Fe(CO)₄. Population of the HOMO decreases while population of the LUMO increases.

decrease in the order



The electron-accepting and -donating capabilities of a ligand can be quantitatively evaluated on the basis of how the populations of the ligand orbitals change in going from a free to a bound ligand. The change in the Mulliken orbital population of the olefins is shown in Figure 2. The depopulation of the π orbital (ligand HOMO) has the following trend: C₂F₄ > C₂H₄ > C₂Cl₄ > C₂Br₄ > C₂I₄ \approx C₂(CN)₄. Except for C₂F₄ and C₂-

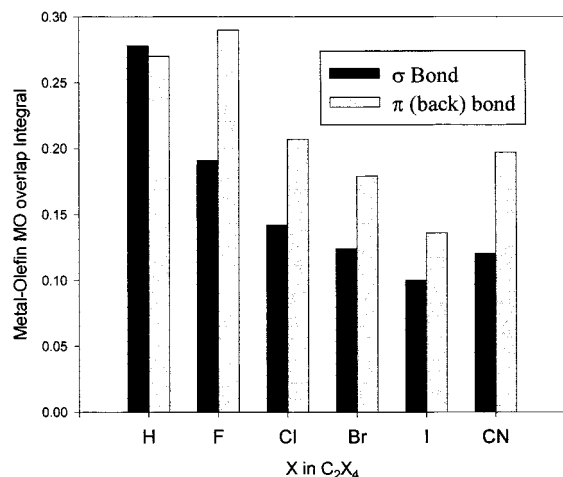


Figure 3. Degree of overlap of the metal-olefin frontier molecular orbital involved in σ and back-bonding (π) interactions in the $\text{Fe}(\text{CO})_4\text{-(C}_2\text{X}_4)$ ($\text{X} = \text{H, F, Cl, Br, I, CN}$) complexes.

(CN)₄, the trend in the π orbital population is not consistent with changes in the HOMO energies. Thus, solely on the basis of the HOMO energies of the ligands relative to ethylene, the halogenated olefins with $\text{X} = \text{Cl, Br, and I}$ would be predicted to be slightly better σ donors than ethylene, but the depopulation of the HOMO indicates that the opposite is occurring. This apparent dichotomy indicates that, as might be anticipated, the ability of a given ligand to donate electron density depends not only on its energy relative to the accepting metal LUMO but also on the overlap between the orbitals. The orbital overlaps are shown in Figure 3. The overlap between the MOs involved in σ bond formation follows the trend $\text{C}_2\text{H}_4 > \text{C}_2\text{F}_4 > \text{C}_2\text{Cl}_4 > \text{C}_2\text{Br}_4 \approx \text{C}_2(\text{CN})_4 > \text{C}_2\text{I}_4$. Thus, the overlap decreases with an increase in the size of both the halogen and, correspondingly, the ligand. As seen in Scheme 1, σ donation involves a σ -dsp hybrid LUMO on the metal. Access to this orbital is impeded by the steric interactions of the axial CO ligands with the halogen substituents on the olefin. Therefore, the degree of orbital overlap involved in σ donation decreases as the olefin gets bulkier. The extent of this steric interaction is reflected in the $\text{C}_{\text{ax}}\text{-Fe-C}_{\text{ax}}$ angle. In response to repulsive forces, the axial CO ligands bend away from the olefin. This can be seen in Scheme 1. As shown in Figure 4 this bending angle correlates with the size of the substituent.

In terms of back-bonding, the π^* orbital population (see Figure 2) follows the trend $\text{C}_2(\text{CN})_4 > \text{C}_2\text{F}_4 > \text{C}_2\text{Cl}_4 > \text{C}_2\text{Br}_4 > \text{C}_2\text{I}_4 > \text{C}_2\text{H}_4$. This trend agrees well with the trend for the change in the energy of the LUMO of the ligands shown in Figure 1. The trend for the overlap (see Figure 3) of the orbitals involved in back-bonding is $\text{C}_2\text{F}_4 > \text{C}_2\text{H}_4 > \text{C}_2\text{Cl}_4 > \text{C}_2(\text{CN})_4 > \text{C}_2\text{Br}_4 > \text{C}_2\text{I}_4$. Clearly, the trend in the orbital overlap does not correlate with the change in population, suggesting that although the π^* orbital of the olefin can be sterically impeded in its approach to the d_{yz} metal orbital, in this case it is the energy gap which largely determines the π -accepting capability.

Because the bonding capabilities of the ligand can depend on both the energy of the orbitals, and the orbital overlap, it is desirable to find a way to evaluate how both factors effect the bonding capabilities of the ligands. For this purpose, a graph has been constructed that illustrates the correlations between these effects (see Figure 5). In Figure 5 the orbital overlap is plotted on the ordinate, while the energy gap between the relevant molecular orbitals is plotted on the abscissa. Efficient ligand metal interaction for either σ -donating or π -accepting ability will be facilitated by large orbital overlaps and small

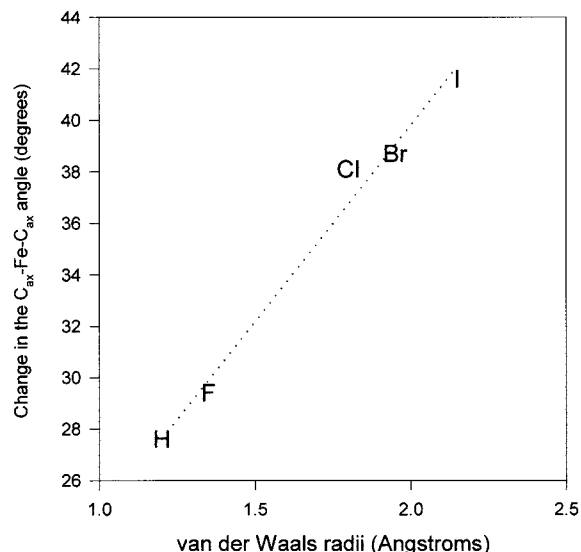


Figure 4. Plot of the van der Waals radii of the olefin substituent vs the change in the $\text{C}_{\text{ax}}\text{-Fe-C}_{\text{ax}}$ angle of the $\text{Fe}(\text{CO})_4(\text{C}_2\text{X}_4)$ ($\text{X} = \text{H, F, Cl, Br, I, CN}$) complexes.

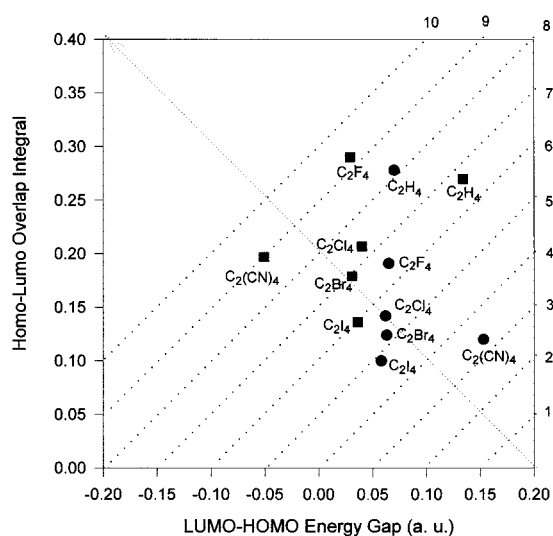


Figure 5. Graph displaying the metal-ligand overlap integral and the FMO energy gaps. Circles (●) are for the σ donation interaction, and squares (■) for the back-bonding interaction. Bonding capabilities increase along the diagonal from the lower right corner to the upper left corner. The numbers on the top and right are not a quantitative measure of bonding but rather indicate the direction of increase in the bonding interactions.

metal-ligand HOMO-LUMO energy gaps. The dotted lines perpendicular to the right to left diagonal can be used to semiquantitatively compare the bonding capability of one ligand with respect to another. On the basis of the location of the ligands in the plot, the σ -donating ability (circles) goes up in the order $\text{C}_2\text{H}_4 > \text{C}_2\text{F}_4 > \text{C}_2\text{Cl}_4 > \text{C}_2\text{Br}_4 > \text{C}_2\text{I}_4 > \text{C}_2(\text{CN})_4$, while the π -accepting ability (squares) follows the order $\text{C}_2\text{F}_4 \approx \text{C}_2(\text{CN})_4 > \text{C}_2\text{Cl}_4 > \text{C}_2\text{Br}_4 > \text{C}_2\text{H}_4 > \text{C}_2\text{I}_4$. Note that the trend for the σ -donating ability agrees better with the trend in orbital overlap than with the trend that would be predicted on the basis of the energy gap between the ligand HOMO and metal fragment LUMO. This suggests that, at least for these complexes, for σ donation, the orbital overlap is the dominant factor in the effective electron-donating capability of a ligand. This is dramatically demonstrated for ethylene and the halogenated olefins, which have very similar ligand HOMO-metal LUMO energy gaps. On the other hand, the trend in the back-bonding

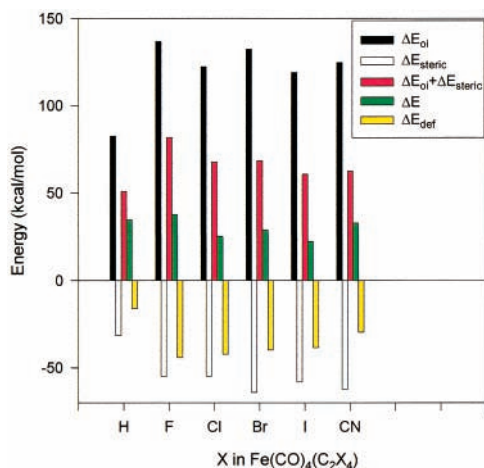


Figure 6. Energy decomposition results for the $\text{Fe}(\text{CO})_4(\text{C}_2\text{X}_4)$ ($\text{X} = \text{H}, \text{F}, \text{Cl}, \text{Br}, \text{I}, \text{CN}$) complexes. ΔE_{oi} = orbital interaction energy, ΔE_{steric} = steric energy, ΔE = total bond energy, and ΔE_{def} = deformation energy.

capability correlates better with the trend in the energy of the ligand LUMO. This is quite obvious for ethylene and tetracyanoethylene, although, in the particular case of C_2Cl_4 relative to C_2Br_4 , where the energy gap is similar, the better overlap for C_2Cl_4 prevails over the slightly more favorable energy gap for C_2Br_4 .

C. Bond Energies of $\text{Fe}(\text{CO})_4(\text{C}_2\text{X}_4)$ Complexes. Figure 6 shows the bond energies calculated from eq 1, as well as the results of the energy decomposition analysis. The trend in bond energy (ΔE_c , kcal/mol) is C_2F_4 (38) > C_2H_4 (35) > $\text{C}_2(\text{CN})_4$ (33) > C_2Br_4 (29) > C_2Cl_4 (25) > C_2I_4 (22). Clearly, the $\text{Fe}-\text{C}_2\text{X}_4$ ($\text{X} = \text{halogens}, \text{CN}$) bond energy is similar to or smaller than the $\text{Fe}-\text{C}_2\text{H}_4$ bond energy. This is opposite what would be predicted by simply considering the σ - and π -bonding capabilities of the olefin. The trend in calculated $\text{Fe}-\text{C}_2\text{X}_4$ ($\text{X} = \text{H}, \text{F}, \text{Cl}$) bond energies agree with prior calculations by Wang and Weitz²⁷ for C_2H_4 , C_2F_4 , and C_2Cl_4 (36, 40, and 30 kcal/mol respectively), although their results are quantitatively somewhat different as they used a different BP86 functional and different basis sets. To our knowledge, in terms of available experimental data, only the bond enthalpy for dissociation of C_2H_4 from $\text{Fe}(\text{CO})_4(\text{C}_2\text{H}_4)$ has been quantitatively and specifically determined experimentally, with a value of 37 ± 3 kcal/mol, as reported by Lewis et al.³⁷ House and Weitz^{35a} estimated a lower limit for the BDE for the $\text{Fe}-\text{C}_2\text{F}_4$ bond in $\text{Fe}(\text{CO})_4(\text{C}_2\text{F}_4)$ of 26 kcal/mol, while Cedeño and Weitz^{35c} estimated the $\text{Fe}-\text{C}_2\text{Cl}_4$ bond enthalpy to be >21 kcal/mol. Bond enthalpies calculated using eq 2 without including BSSE are 31, 36, and 25 kcal/mol for C_2H_4 , C_2F_4 , and C_2Cl_4 , respectively, which are compatible with the available experimental data. As previously indicated, inclusion of the BSSE correction leads to somewhat lower values for these BDEs, but the trend in BDEs is unaffected.

The results from the energy decomposition analysis indicate that the total electronic interaction energy ($\Delta E_{oi} + \Delta E_{steric}$) has the following trend: $\text{C}_2\text{F}_4 > \text{C}_2\text{Br}_4 > \text{C}_2\text{Cl}_4 > \text{C}_2(\text{CN})_4 > \text{C}_2\text{I}_4 > \text{C}_2\text{H}_4$. The strong interaction between the halogenated olefins and tetracyanoethylene and the metal carbonyl fragment is due to the large orbital interaction energy (ΔE_{oi}). The trend in this energy term is similar to the trend in $\Delta E_{oi} + \Delta E_{steric}$. It also follows the trend in electronegativity of the substituent, which is what would be expected in the context of the DCD model. Furthermore, the differences in ΔE_{oi} between the halogenated species and ethylene are larger than the differences in the steric

(repulsive) term (ΔE_{steric}) among these ligands. The steric term (ΔE_{steric}), which is composed of the orbital repulsion term (ΔE_{pauli}) and the electrostatic interaction term (ΔE_{elst}), has the trend $\text{C}_2\text{Br}_4 > \text{C}_2(\text{CN})_4 > \text{C}_2\text{I}_4 > \text{C}_2\text{Cl}_4 \approx \text{C}_2\text{F}_4 > \text{C}_2\text{H}_4$. Interestingly, steric repulsion is larger for Br as a substituent than it is for I, despite the fact that I is a larger substituent. This is due to the differences in C–X bond length and C–X out of plane angles, which lead to the iodine substituents being further from the CO ligands. The orbital repulsion portion (ΔE_{pauli}) of the steric energy term dominates the overall trend in the magnitude of this term; that is, $\text{C}_2\text{Br}_4 > \text{C}_2\text{I}_4 > \text{C}_2\text{Cl}_4 > \text{C}_2\text{F}_4 > \text{C}_2(\text{CN})_4 > \text{C}_2\text{H}_4$. As expected, the halogens, with their larger orbitals, have larger orbital repulsion than the carbon in CN and the hydrogens in C_2H_4 . The trend in the steric energy is parallel to the trend observed for the change in the $\text{C}_{ax}-\text{Fe}-\text{C}_{ax}$ angle: The larger the steric term, the more the axial CO ligands bend away from the olefin.

However, we feel that the most important result that comes out of the decomposition analysis of the metal–olefin bond energy involves the deformation energy. *If only the total interaction energy ($\Delta E_{oi} + \Delta E_{steric}$) were considered, all the halogenated olefins would be more strongly bound to $\text{Fe}(\text{CO})_4$ than ethylene.* This is what would be expected on the basis of the Dewar–Chatt–Duncanson model. In the context of the DCD model, the increase in the back-bonding ability of the halogenated ligands is expected to contribute to larger bond strengths for the haloolefin complexes relative to the ethylene complex. However, this is not consistent with the calculated bond energy (ΔE_c). This is because the deformation energy is the energetic factor that effectively determines the trend in Fe –olefin bond strengths. As pointed out in a prior paper on this subject,¹³ the deformation of the reacting moieties can be an important factor in determining bond dissociation energies, yet with some exceptions,^{1,26,57–61} it has typically been neglected in considerations of bonding and expectations regarding BDEs in organometallic complexes.

Another interesting result derived from these calculations is that the metal–olefin bond lengths do not correlate directly with the bond energy for all the complexes being studied. The $\text{Fe}-\text{C}_2\text{H}_4$ bond is the longest, but the $\text{Fe}-\text{C}_2\text{H}_4$ bond energy is larger than the $\text{Fe}-\text{C}_2\text{Cl}_4$ bond energy, despite the fact that the $\text{Fe}-\text{C}_2\text{Cl}_4$ bond length is almost 0.1 Å shorter than the $\text{Fe}-\text{C}_2\text{H}_4$ bond length. Thus, typical expectations regarding bond energy–bond order correlations are not valid for this series of complexes and, more importantly, it is clear that predictions of relative bond energy based on relative bond lengths could be inaccurate.

D. Analysis of the Deformations. As seen in Scheme 1, both the metal fragment and the olefin deform significantly. Figure 7 shows the contributions of the deformation of $\text{Fe}(\text{CO})_4$ and the olefin to the total deformation energy. Compared to the deformation energy for $\text{Fe}(\text{CO})_4$ in the ethylene complex, the $\text{Fe}(\text{CO})_4$ fragments in the other olefin complexes have 5–6 kcal/mol larger deformation energies. As shown in Figure 4, the extent of bending of the axial CO ligands away from the olefin is larger for the substituted olefins than it is for ethylene. The change in the $\text{C}_{ax}-\text{Fe}-\text{C}_{ax}$ bending angle correlates with the size of the substituent around the olefin, increasing with an increase in the van der Waals radii of the substituent. However, the deformation energy of the $\text{Fe}(\text{CO})_4$ fragment cannot be correlated directly to the degree of bending, because it is also influenced by changes in the $\text{Fe}-\text{C}-\text{O}$ (especially for axial COs) and $\text{C}_{eq}-\text{Fe}-\text{C}_{eq}$ bond angles, as well as in the $\text{Fe}-\text{C}$ bond lengths.

The deformation of the bound olefin accounts for more than half of the total deformation energy. Interestingly, the deforma-

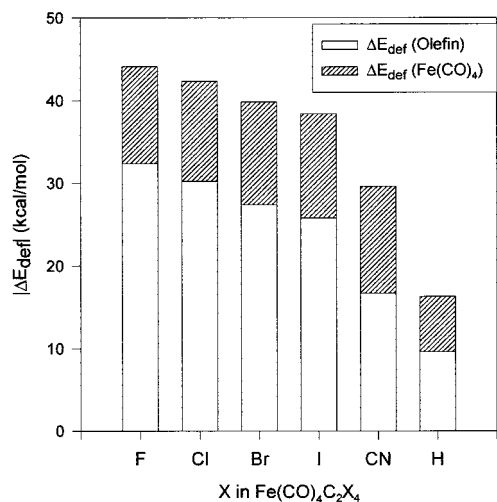


Figure 7. Contributions of the deformation of the $\text{Fe}(\text{CO})_4$ moiety and the olefin to the total deformation energy.

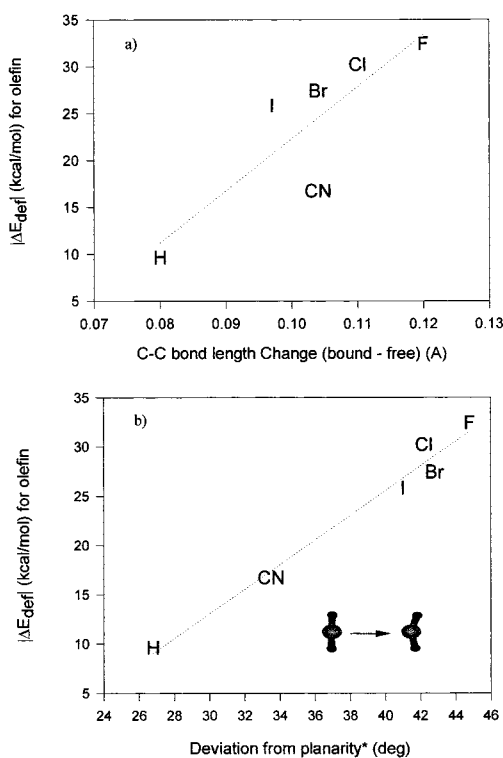


Figure 8. Deformation energy of the olefin as a function of changes in the geometry of C_2X_4 upon bonding to the metal: (a) change in the olefin C–C bond length; (b) deviation from planarity.

tion energy of the olefin correlates rather well with both the elongation of the C–C bond length and the olefin's deviation from planarity. The latter quantity is measured by the angle between the substituent and the plane of the double bond (see Figure 8b). Because both parameters are related to the hybridization of the carbon atoms in the ligand, the results suggest that the bonding of the olefin to iron leads to a change in the hybridization of the olefin carbon atoms from sp^2 toward sp^3 character. The change in hybridization is a result of the increase in population of the olefin's π^* antibonding orbital. It is populated at the expense of the olefin π orbital. Furthermore, an increase in the electronegativity or the electron-withdrawing nature of the olefinic substituents increases the population of the π^* orbital, which effectively changes the hybridization. This is shown in Figure 9, where the average C=C bond order

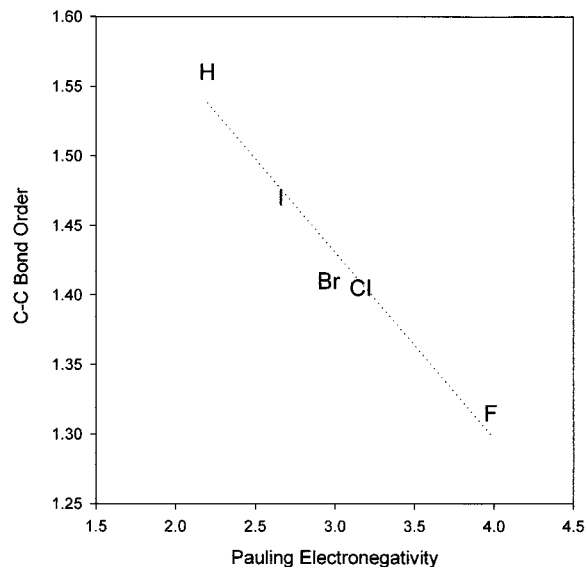


Figure 9. Calculated C–C bond order for the bound olefins as a function of the Pauling electronegativity⁶² of the substituent on the olefin.

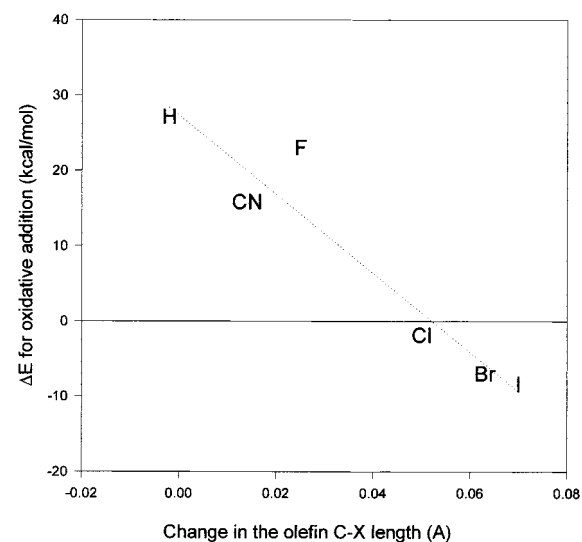
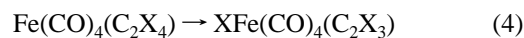


Figure 10. Plot showing the correlation between the change in the C–X bond length in the olefin and the calculated ΔE for the reaction $\text{Fe}(\text{CO})(\text{C}_2\text{X}_4) \rightarrow \text{XFe}(\text{CO})_4(\text{C}_2\text{X}_3)$.

calculated from the populations of the ligand orbitals and the deviation from planarity is plotted against the electronegativity⁶² of the substituent.

Finally, and as a result of the rehybridization of the olefinic carbons, the C–X bond length in the olefin also changes on bonding. Recently, Cedeño and Weitz^{35c} found that $\text{Fe}(\text{CO})_4(\text{C}_2\text{Cl}_4)$ undergoes an oxidative addition process in the gas phase to form $\text{ClFe}(\text{CO})_4(\text{C}_2\text{Cl}_4)$. Motivated by this observation, the ΔE_{rxn} 's for the oxidative addition reactions,



were calculated. Interestingly, as seen in Figure 10, the change in the C–X bond length in the monoolefin correlates well with the calculated ΔE_{rxn} . Upon bonding, the C–X bond in the olefin lengthens (for X = halogen). The more the C–X bond stretches, the more thermodynamically favorable the oxidative addition process becomes. This implies that bonding of the olefin to the metal leads to a decrease in energy of the C–X bond in the

TABLE 3: Calculated Geometries for ${}^3\text{Fe}(\text{CO})_4$ and Free Olefins (C_2X_4)^a

${}^3\text{Fe}(\text{CO})_4$							
Fe–C _{ax}	Fe–C _{eq}	C–O _{ax}	C–O _{eq}	C _{ax} –Fe–C _{ax}	C _{eq} –Fe–C _{eq}	Fe–CO _{ax}	Fe–C–O _{eq}
1.845	1.806	1.153	1.155	149.8	97.8	177.9	179.8
Free Olefins							
param	X =						
	H	F	Cl	Br	I	CN	
C–C	1.334	1.333	1.355	1.346	1.347	1.384	
C–X	1.091	1.329	1.742	1.929	2.125	1.425	
X–C–X	121.8	113.5	115.4	114.0	113.0	117.1	

^a Bond lengths in Å; angles in deg.

olefin. Of course, the energetics of the oxidative addition reaction also depends on the energy of the other bonds being formed and broken during the reaction. On the basis of these arguments, even though it has not been reported, it is highly likely that an oxidative addition reaction will occur in the $\text{Fe}(\text{CO})_4(\text{C}_2\text{I}_4)$ complex to form $\text{IFe}(\text{CO})_4(\text{C}_2\text{I}_3)$.

Conclusions

The bond dissociation energies (ΔE_c) for the $\text{Fe}-\text{C}_2\text{X}_4$ bond in the olefin complexes $\text{Fe}(\text{CO})_4(\text{C}_2\text{X}_4)$ were calculated using a DFT method with the BP86 functional as 35, 38, 25, 29, 22, and 33 kcal/mol for X = H, F, Cl, Br, I, and CN, respectively (without BSSE correction). The calculated bond enthalpy (ΔH_{298}) for ethylene, of 31 kcal/mol, is close to but slightly lower than the experimentally determined value of 37 ± 3 kcal/mol.³⁶ Those for the perfluoroethylene (36 kcal/mol) and perchloroethylene (25 kcal/mol) complexes are compatible with the experimental lower limit values established by Weitz and co-workers^{35a,c} (26 and 21 kcal/mol for X = F and Cl, respectively). Inclusion of the BSSE correction lowers these values further but does not change the overall trend in BDEs: the $\text{Fe}-\text{C}_2\text{F}_4$ BDE is predicted to be either slightly larger or comparable to the $\text{Fe}-\text{C}_2\text{H}_4$ BDE, and the $\text{Fe}-\text{C}_2\text{Cl}_4$ BDE is smaller than the BDE of either of these complexes.

When the bonding of ethylene and the substituted olefins is analyzed in the context of the Dewar–Chatt–Duncanson model, the iron–olefin bonding interactions are expected to be stronger for the halogenated olefins and tetracyanoethylene complexes than for ethylene. On the basis of these factors alone, the bond strength would be expected to increase as the electron-withdrawing capability of the substituent on the olefin increases. An energy decomposition analysis indicates that, in agreement with the Dewar–Chatt–Duncanson model, the electronic interactions between the haloolefins and tetracyanoethylene and $\text{Fe}(\text{CO})_4$ are larger than between $\text{Fe}(\text{CO})_4$ and ethylene, mainly as a result of an increase in the degree of back-donation. However, the formation of these adducts requires the *deformation of both C_2X_4 (X = H, halogens, CN) and $\text{Fe}(\text{CO})_4$* . The energy necessary to effect this deformation results in a decrease in the bond dissociation energy relative to that calculated taking into account *only* the electronic factors involved in bonding (the σ -donating, π -accepting, and steric interactions). It has been previously reported that in the $\text{Fe}(\text{CO})_{5-n}(\text{N}_2)_n$ ($n = 1-5$) complexes the deformation energy is the determining factor in the trend in the bond dissociation energy in this series.¹³ The present study provides another situation where *the deformation energy is the determining factor in the trend in the bond dissociation energy in a homologous series of complexes*. The $\text{Fe}(\text{CO})_4$ fragment deforms by bending the axial CO ligands away from the olefin. The magnitude of the bending angle

increases with the size of the olefin substituent (X). However, most of the deformation energy (>55%) goes into deformation of the olefin, which involves a change in the hybridization of the olefinic carbon from sp^2 in the free olefin toward an sp^3 -like carbon in the bound olefin. The change in hybridization correlates with an increase in the electronegativity of the substituent. Interestingly, for all X except X = H, the C–X bond length increases (Table 3) and the C–X bond energy gets smaller (relative to the free olefin) when the olefin is bound to the metal. The increase in the C–X bond length correlates with the calculated change in the energetics of the oxidative addition reaction of $\text{Fe}(\text{CO})_4(\text{C}_2\text{X}_4)$ to produce $\text{XFe}(\text{CO})_4(\text{C}_2\text{X}_3)$.

The effect of the deformation of the olefin, and the metal fragment, on the metal–olefin bond energies has received considerably less attention than the effect of orbital interactions, steric repulsion, and electrostatics. The results of this study, for the $\text{Fe}(\text{CO})_4(\text{C}_2\text{X}_4)$ complexes (X = H, halogens, CN), again demonstrate that the deformation energy can play a controlling role in trends in the BDEs in a homologous series of complexes. As such, it should be clear that, at least in some situations, the deformation energy *must* be considered for a series of complexes in order to obtain a complete and consistent picture of bonding and trends in BDEs.

Acknowledgment. We acknowledge the support of this work by the National Science Foundation under Grant NSF 97-34891.

References and Notes

- (1) Marks, T. J. In *Bonding Energetics in Organometallic Compounds*; ACS Symposium Series 428; Marks, T. J., Ed.; American Chemical Society: Washington, DC, 1990.
- (2) Laird, B. B.; Ross, R. B.; Ziegler, T. In *Chemical Applications of Density Functional Theory*; ACS Symposium Series 629; Laird, B. B., Ross, R. B., Ziegler, T., Eds.; American Chemical Society: Washington, DC, 1996.
- (3) *Density Functional Methods in Chemistry*; Labanowsky, J. K., Andzelm, J. W., Eds.; Springer-Verlag: New York, 1991.
- (4) (a) Ziegler, T. *Chem. Rev.* **1991**, *91*, 651. (b) Ziegler, T. *Can. J. Chem.* **1995**, *73*, 743.
- (5) van Wüllen, C. *J. Chem. Phys.* **1996**, *105*, 5485.
- (6) Wang, W.; Weitz, E. *J. Phys. Chem.* **1997**, *101*, 2358.
- (7) Rosa, A.; Ehlers, A. W.; Baerends, E. J.; Snijders, J. G.; te Velde, G. *J. Phys. Chem.* **1996**, *100*, 5690.
- (8) Li, J.; Schreckenbach, G.; Ziegler, T. *J. Am. Chem. Soc.* **1995**, *117*, 486.
- (9) Radius, U.; Bickelhaupt, F. M.; Ehlers, A. W.; Goldberg, N.; Hoffmann, R. *Inorg. Chem.* **1998**, *37*, 1080.
- (10) Delley, B.; Wrinn, M.; Luthi, H. P. *J. Chem. Phys.* **1994**, *100*, 5785.
- (11) Ehlers, A. W.; Frenking, G. *Organometallics* **1995**, *14*, 423.
- (12) Ehlers, A. W.; Frenking, G. *J. Am. Chem. Soc.* **1994**, *116*, 1514.
- (13) Cedeño, D. L.; Weitz, E.; Bérces, A. *J. Phys. Chem. A* **2001**, *105*, 3773.
- (14) (a) Ziegler, T.; Rauk, A. *Theor. Chim. Acta* **1977**, *46*, 1. (b) Ziegler, T.; Rauk, A. *Inorg. Chem.* **1979**, *18*, 1558. (c) Ziegler, T.; Rauk, A. *Inorg. Chem.* **1979**, *18*, 1755.
- (15) Bickelhaupt, F. M.; Nibbering, N. M.; van Wezenbeek, E. M.; Baerends, E. J. *J. Phys. Chem.* **1992**, *96*, 4864.

- (16) (a) Morokuma, K. *Acc. Chem. Res.* **1977**, *10*, 294. (b) Kitaura, K.; Morokuma, K. *Int. J. Quantum Chem.* **1976**, *10*, 325.
- (17) Collman, J. P.; Hegedus, L. S.; Norton, J. R.; Finke, R. G. *Principles and Applications of Organotransition Metal Chemistry*; University Science Books: Mill Valley, CA, 1987.
- (18) Crabtree, R. H. *The Organometallic Chemistry of Transition Metals*; Wiley: New York, 1986. For the DCD model, see p 107.
- (19) Yamamoto, A. *Organotransition Metal Chemistry*; Wiley: New York, 1986.
- (20) Geoffroy, G. L.; Wrighton, M. S. *Organometallic Photochemistry*; Academic Press: New York, 1979.
- (21) Dewar, M. J. S. *Bull. Chem. Soc. Fr.* **1951**, *18*, C79.
- (22) Chatt, J.; Duncanson, L. A. *J. Chem. Soc.* **1953**, 2939.
- (23) Pruchnik, F. P. *Organometallic Chemistry of the Transition Elements*; Plenum Press: New York, 1990. For the DCD model, see p 343.
- (24) Tollman, C. A. *J. Am. Chem. Soc.* **1974**, *96*, 2780.
- (25) Nunzi, F.; Sgamellotti, A.; Re, N.; Floriani, C. *J. Chem. Soc., Dalton Trans.* **1999**, 3487.
- (26) (a) Frenking, G.; Pidun, U. *J. Chem. Soc., Dalton Trans.* **1997**, 3487. (b) Uddin, J.; Dapprich, S.; Frenking, G.; Yates, B. F. **1999**, *18*, 457.
- (27) Wang, W.; Weitz, E. Unpublished results. DFT calculations were performed using Gaussian 94; the BP86 used was similar to the one described here, except that it uses Perdew's 81 as the local density functional instead of that by Volko et al.
- (28) *Comprehensive Organometallic Chemistry*; Wilkinson, G. W., Stone, F. G. A., Abel, E. W., Eds.; Pergamon Press: Oxford, U.K.; Vol. 4.
- (29) Wu, Y.; Bentsen, J. G.; Brinkley, C. G.; Wrighton, M. S. *Inorg. Chem.* **1987**, *26*, 530.
- (30) (a) Fields, R.; Germain, M. M.; Haszeldine, R. N.; Wiggans, P. W. *J. Chem. Soc. A* **1970**, 1969. (b) Fields, R.; Godwin, G. L.; Haszeldine, R. N. *J. Chem. Soc., Dalton Trans.* **1975**, 1867.
- (31) (a) Miller, M. E.; Grant, E. R. *J. Am. Chem. Soc.* **1985**, *107*, 3386. (b) Weiller, B. H.; Miller, M. E.; Grant, E. R. *J. Am. Chem. Soc.* **1987**, *109*, 352.
- (32) Darensbourg, D. J.; Nelson, H. H., III.; Hyde, C. L. *Inorg. Chem.* **1974**, *13*, 2135.
- (33) Fleckner, H.; Grevels, F. W.; Hess, D. *J. Am. Chem. Soc.* **1984**, *106*, 2027.
- (34) Wilson, S. T.; Coville, N. J.; Shapely, J. R.; Osborn, J. A. *J. Am. Chem. Soc.* **1974**, *96*, 4038.
- (35) (a) House, P. G.; Weitz, E. *J. Phys. Chem. A* **1997**, *101*, 2988. (b) Long, G. T.; Weitz, E. *J. Am. Chem. Soc.* **2000**. (c) Cedeño, D. L.; Weitz, E. *J. Phys. Chem. A* **2000**, *104*, 8011.
- (36) Lewis, K. E.; Golden, D. M.; Smith, G. P. *J. Am. Chem. Soc.* **1984**, *106*, 3905.
- (37) *Jaguar 4.0*; Schrödinger, Inc.: Portland, OR, 1998–1999.
- (38) (a) Friesner, R. A. *Chem. Phys. Lett.* **1985**, *116*, 39. (b) Friesner, R. A. *J. Chem. Phys.* **1987**, *86*, 3522. (c) Friesner, R. A. *J. Phys. Chem.* **1988**, *92*, 3091. (d) Langlois, J. M.; Muller, R. P.; Coley, T. R.; Goddard, W. A., III.; Ringnalda, M. N.; Won, Y.; Friesner, R. A. *J. Chem. Phys.* **1990**, *92*, 7488. (e) Ringnalda, M. N.; Belhadj, M.; Friesner, R. A. *J. Chem. Phys.* **1990**, *93*, 3397. (f) Friesner, R. A. *Annu. Rev. Phys. Chem.* **1991**, *94*, 8152.
- (39) Slater, J. C. *Quantum Theory of Molecules and Solids, Vol. 4: The Self-Consistent Field for Molecules and Solids*; McGraw-Hill: New York, 1974.
- (40) Vosko, S. H.; Wilk, L.; Nusair, M. *Can. J. Phys.* **1980**, *58*, 1200.
- (41) Becke, A. D. *Phys. Rev. A* **1988**, *38*, 3098.
- (42) (a) Perdew, J. P. *Phys. Rev. B* **1986**, *33*, 8822. (b) Perdew, J. P. *Phys. Rev. B* **1986**, *34*, 7406.
- (43) Hay, P. J.; Wadt, W. R. *J. Chem. Phys.* **1985**, *82*, 299.
- (44) (a) Ditchfield, R.; Hehre, W. J.; Pople, J. A. *J. Chem. Phys.* **1971**, *54*, 724. (b) Hehre, W. J.; Pople, J. A. *J. Chem. Phys.* **1972**, *56*, 4233. (c) Binkley, J. S.; Pople, J. A. *J. Chem. Phys.* **1977**, *66*, 879. (d) Hariharan, P. C.; Pople, J. A. *Theor. Chim. Acta* **1973**, *28*, 213. (e) Hehre, W. J.; Ditchfield, R.; Pople, J. A. *J. Chem. Phys.* **1972**, *56*, 2257. (f) Francl, M. M.; Pietro, W. J.; Hehre, W. J.; Binkley, J. S.; Gordon, M. S.; DeFrees, D. J.; Pople, J. A. *J. Chem. Phys.* **1982**, *77*, 3654.
- (45) Poliakov, M.; Weitz, E. *Acc. Chem. Res.* **1987**, *20*, 408.
- (46) Deakne, C. A.; Liebman, J. F. In *Encyclopedia of Computational Chemistry*; Schleyer, P. v. R., Allinger, N. R., Clark, T., Gasteiger, J., Kollman, P. A., Schaefer, H. F., III., Schreiner, P. R., Eds.; Wiley: Chichester, U.K., 1998; Vol. 2, pp 1439.
- (47) Boys, S. F.; Bernardi, F. *Mol. Phys.* **1970**, *19*, 553.
- (48) Cedeño D. L.; Weitz E. Results to be published.
- (49) Davidson, E. R.; Chakravorty, S. *J. Chem. Phys. Lett.* **1994**, *217*, 48.
- (50) (a) *Amsterdam Density Functional, ADF99, SCM*; Vrije Universiteit: Vrije, The Netherlands. (b) Baerends, E. J.; Ellis, D. E.; Ros, P. *Chem. Phys.* **1973**, *2*, 41. (c) Versluis, L.; Ziegler, T. *J. Chem. Phys.* **1988**, *88*, 322. (d) te Velde, G.; Baerends, E. J. *Theor. Chem. Acc.* **1998**, *99*, 391. (e) Fonseca Guerra, C.; Snijders, J. G.; te Velde, G.; Baerends, E. J. *Theor. Chem. Acc.* **1998**, *99*, 391.
- (51) (a) Snijders, G. J.; Baerends, E. J.; Vernooijs, P. *At. Data Nucl. Data Tables* **1982**, *26*, 483. (b) Vernooijs, P.; Snijders, G. J.; Baerends, E. J. *Slater Type Basis Functions for the whole Periodic System*; Internal Report; Free University of Amsterdam: Amsterdam, The Netherlands, 1981.
- (52) Krijn, J.; Baerends, E. J. *Fit functions in the HFS-method*; Internal Report; Free University of Amsterdam: Amsterdam, The Netherlands, 1984.
- (53) Mulliken, R. S. *J. Chem. Phys.* **1955**, *48*, 1833.
- (54) Davis, M. I.; Speed, C. S. *J. Organomet. Chem.* **1970**, *21*, 401.
- (55) Beagley, B.; Schmidling, D. G.; Cruickshank, D. W. J. *Acta Crystallogr.* **1973**, *B29*, 14.
- (56) (a) Rossi, A. R.; Hoffmann, R. *Inorg. Chem.* **1975**, *14*, 365. (b) Elian, M.; Hoffmann, R. *Inorg. Chem.* **1975**, *14*, 1058.
- (57) Martinho Simões, J. A.; Beauchamp, J. L. *Chem. Rev.* **1990**, *90*, 629.
- (58) Pilcher, G. *Pure Appl. Chem.* **1989**, *61*, 855.
- (59) Comba, P. *Coord. Chem. Rev.* **1993**, *123*, 1.
- (60) Michalak, A.; Ziegler, T. *Organometallics* **2000**, *19*, 1850.
- (61) Cui, Q.; Musaev, D. G.; Morokuma, K. *Organometallics* **1997**, *16*, 1355.
- (62) *CRC Handbook of Chemistry and Physics*; Lide, D. R., Ed.; CRC Press: Boca Raton, FL, 1999–2000.